

# MEASUREMENT OF THE PION FORMFACTOR WITH KLOE AND STUDY OF THE REACTION $f_0(980) \rightarrow \pi^+\pi^-$

The KLOE collaboration <sup>a</sup>

represented by Achim Denig

*Universität Karlsruhe, IEKP, Postfach 3640, 76021 Karlsruhe, Germany*

At the Frascati  $\phi$ -factory DAΦNE the pion formfactor is measured by means of the 'radiative return', i.e. by using events in which one of the collider electrons (positrons) has radiated an initial state radiation photon, lowering in such a way the invariant mass  $M_{\pi\pi}$  of the two-pion-system. In a recent publication of the KLOE collaboration the initial state radiation photon had been required to be at small polar angles with respect to the beam axis. We are presenting results from a new and complementary analysis in which the photon is tagged at large polar angles. Only like this the threshold region  $M_{\pi\pi}^2 < 0.35\text{GeV}^2$  becomes accessible. Moreover, the final state  $\pi^+\pi^-\gamma$  allows to study the  $\phi$  radiative decay into the scalar particle  $f_0(980)$  with  $f_0(980) \rightarrow \pi^+\pi^-$ . For the first time the two-pion mass spectrum could be fitted with different theoretical models for the description of this  $\phi$  radiative decay.

## 1 The radiative return and its connection to the muon anomaly

Precision measurements of the cross section for  $e^+e^-$  annihilation into hadrons are of utmost importance for an interpretation of the recent measurement of the anomalous magnetic moment of the muon  $a_\mu$  at the Brookhaven National Laboratory (experiment E821, 0.5 ppm accuracy)<sup>1</sup>. A comparison of the E821 measurement with the theory prediction allows a unique test of the standard model of particle physics. The theory prediction is however limited by the hadronic contribution  $a_\mu^{\text{hadr}}$  and can only be derived by means of a dispersion integral, using hadronic cross section data as input<sup>2,3</sup>. The process  $e^+e^- \rightarrow \pi^+\pi^-$  below 1 GeV is of special importance since it contributes to  $\sim 60\%$  to the total integral.

Recently it could be shown that at particle factories, such as DAΦNE or the B-factories, which are operated at a constant center-of-mass energy  $\sqrt{s}$ , the hadronic cross section becomes accessible over a wide energy range  $< \sqrt{s}$  using events with initial state radiation (ISR), lowering in such a way the invariant mass of the hadronic system  $M_{\text{hadr}}$  (so-called 'radiative return'). The

---

<sup>a</sup>The KLOE Collaboration: F. Ambrosino, A. Antonelli, M. Antonelli, C. Bacci, P. Beltrame, G. Bencivenni, S. Bertolucci, C. Bini, C. Bloise, S. Bocchetta, V. Bocci, F. Bossi, D. Bowring, P. Branchini, R. Caloi, P. Campana, G. Capon, T. Capussela, F. Ceradini, S. Chi, G. Chiefari, P. Ciambone, S. Conetti, E. De Lucia, A. De Santis, P. De Simone, G. De Zorzi, S. Dell'Agnello, A. Denig, A. Di Domenico, C. Di Donato, S. Di Falco, B. Di Micco, A. Doria, M. Dreucci, G. Felici, A. Ferrari, M. L. Ferrer, G. Finocchiaro, S. Fiore, C. Forti, P. Franzini, C. Gatti, P. Gauzzi, S. Giovannella, E. Gorini, E. Graziani, M. Incagli, W. Kluge, V. Kulikov, F. Lacava, G. Lanfranchi, J. Lee-Franzini, D. Leone, M. Martini, P. Massarotti, W. Mei, L. Meola, S. Miscetti, M. Moulson, S. Müller, F. Murtas, M. Napolitano, F. Nguyen, M. Palutan, E. Pasqualucci, A. Passeri, V. Patera, F. Perfetto, L. Pontecorvo, M. Primavera, P. Santangelo, E. Santovetti, G. Saracino, B. Sciascia, A. Sciubba, F. Scuri, I. Sfligoi, T. Spadaro, M. Testa, L. Tortora, P. Valente, B. Valeriani, G. Venanzoni, S. Veneziano, A. Ventura, R. Versaci, G. Xu.

KLOE collaboration could prove for the two-pion-channel (pion formfactor) that this method is not only complementary but also competitive with the standard energy scan method<sup>4</sup>. The results of the published KLOE measurement, a comparison with recent precision data from the VEPP-2M collider in Novosibirsk and the implications for the muon anomaly can be summarized as follows:

- In the published KLOE analysis events have been selected, in which the ISR-photon is emitted at small (large) polar angles  $\Theta_\gamma < 15^\circ$  and  $\Theta_\gamma > 165^\circ$  with respect to the beam axis. The photon cannot be tagged in such an approach (so-called *untagged analysis*).
- From the radiative cross section  $e^+e^- \rightarrow \pi^+\pi^-\gamma$  the non-radiative cross section  $e^+e^- \rightarrow \pi^+\pi^-$  (pion formfactor) has been extracted using a radiator function (obtained from the Monte-Carlo generator PHOKHARA<sup>5</sup>) for the theoretical description of the ISR-process. The total systematic error of 1.3% for the pion formfactor includes contributions from the experimental side (e.g. efficiencies, background, in total 0.9%) and from the theory side (e.g. radiator function, Bhabha cross section for normalization, in total 0.9%).
- The pion formfactor measured by KLOE is in fair agreement with measurements coming from the Novosibirsk collider VEPP-2M (experiments CMD-2<sup>6</sup> and SND<sup>7</sup>), where an energy scan has been performed. Please notice that the SND data have come closer to the KLOE spectrum at high masses above the  $\rho$  peak, only after the correct treatment of the radiative corrections in the SND analysis, even though a systematic shift of few percent is still visible.
- All three experiments CMD-2, KLOE and SND show large deviations of up to 15% in the mass range above the  $\rho$  peak with respect to spectral functions obtained from hadronic  $\tau$  decays, which can be related to the  $\pi^+\pi^-$  cross section by means of the conserved vector current (CVC) theorem and after correcting for isospin breaking effects. The origin of the deviation between  $e^+e^-$ - and  $\tau$ -data is not understood.
- The contribution of the two-pion channel to the dispersion integral for  $a_\mu^{\text{hadr}}$  has been computed with KLOE data. In the mass range  $0.35 < M_{\pi\pi}^2 < 0.95\text{GeV}^2$  the value for  $a_\mu^{\pi\pi}$  is  $(388.7 \pm 0.8_{\text{stat}} \pm 3.5_{\text{syst}} \pm 3.5_{\text{theo}}) \times 10^{-10}$ . CMD-2 and SND agree in the dispersion integral within 0.5 standard deviations with the KLOE measurement<sup>b</sup>.

## 2 Radiative return with tagged photons

The analysis described above, in which the ISR-photon is emitted at small polar angles, does not allow to cover the threshold region  $M_{\pi\pi}^2 < 0.35\text{GeV}^2$ , since in this kinematical region the two tracks are emitted essentially back-to-back to the ISR-photon and hence cannot be detected simultaneously in the fiducial volume defined for the pion tracks  $50^\circ < \Theta_\pi < 130^\circ$ . In order to measure the pion formfactor at threshold, we are now performing a complementary analysis, in which the ISR-photon is tagged at large polar angles  $50^\circ < \Theta_\gamma < 130^\circ$ . Due to the  $1/s^2$  dependence in the dispersion integral for  $a_\mu^{\text{hadr}}$ , the low mass region of the two-pion cross section is actually giving a  $\sim 20\%$  contribution to the total integral and hence an improved determination of the cross section at threshold is needed. The tagged photon analysis allows also a very valuable cross check of the  $\rho$  peak region, which was covered in the published small angle analysis. It should be noted that new analysis tools are used and that the radiator function and FSR corrections are different. In the following we comment on the status of the analysis and the specific requirements for the tagged analysis.

---

<sup>b</sup>in the somewhat smaller range  $0.37 < M_{\pi\pi}^2 < 0.93\text{GeV}^2$

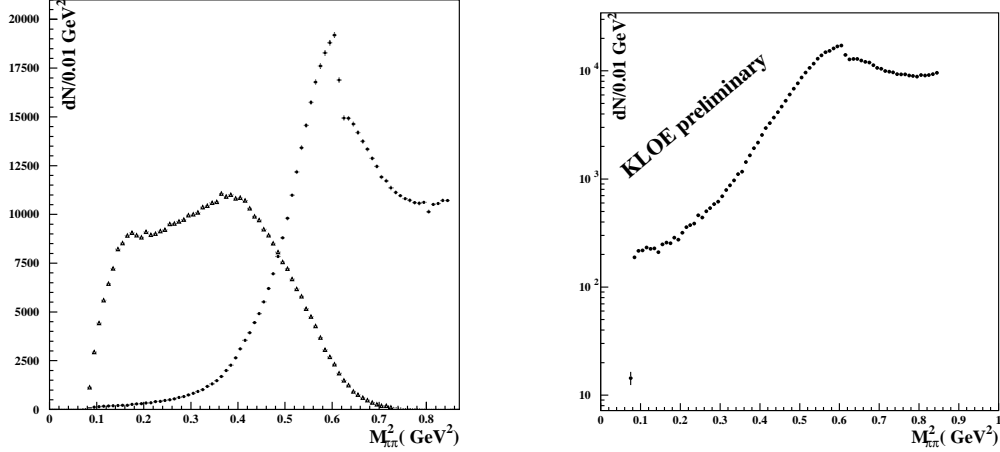


Figure 1: *Left: Mass spectrum for signal events  $\pi^+\pi^-\gamma$  (circles) as expected by Monte-Carlo simulation after the application of the acceptance cuts. Background from  $\phi \rightarrow \pi^+\pi^-\pi^0$  (triangles) is dominating the low mass region. Right: Mass spectrum from data after the full analysis chain. The large background from  $\phi \rightarrow \pi^+\pi^-\pi^0$  can be removed by means of dedicated selection cuts.*

- The cross section for large angle photon events is approximately a factor 5 smaller than for small angle events. Especially in the low  $M_{\pi\pi}$  region, where the pion formfactor is getting rather small, statistics becomes an issue. We use the data taken in 2002, which corresponds to an integrated luminosity of  $\sim 240\text{pb}^{-1}$ . Like this we select  $\sim 45000$  large angle photon events.
- At large photon angles background from  $\phi \rightarrow \pi^+\pi^-\pi^0$  is large, especially in the low  $M_{\pi\pi}$  region as can be seen in fig. 1(left). However, due to the fact that the ISR-photon is tagged and the event kinematics is closed, it is possible to apply stringent cuts to reduce this kind of background. We ask the angle of the missing momentum - calculated from the two pion tracks - to be within a certain window close to the angle of the tagged photon. For  $\pi^+\pi^-\gamma$  events this angle is expected to be  $\sim 0^\circ$ , while for  $\pi^+\pi^-\pi^0$  events it has a broad distribution peaked at  $\Omega \approx 20^\circ$ . Moreover, we perform a kinematic fit in the hypothesis of the background channel  $\pi^+\pi^-\pi^0$ , using four-momentum conservation and the  $\pi^0$  mass as constraints, and cut on  $\chi_{\pi\pi\pi}^2$ .
- Another important background arises from events, in which the photon is not emitted from the initial electrons or positrons, but from the pions (final state radiation, FSR). In the radiative return these kind of events are a background and have to be cut from Monte-Carlo simulation. We use the PHOKHARA code<sup>5</sup>, in which the model of scalar QED (pointlike pions) is used for the estimate of FSR, and in which FSR-corrections up to NLO are considered. Within this model we find a contribution from FSR at large  $M_{\pi\pi}$  of up to 20%. The model assumption of scalar QED can be tested by means of the forward-backward asymmetry (see below), which arises from the ISR-FSR-interference and has been found to describe well the data with a precision of better than few percent.
- Beneath FSR, a further irreducible background is coming from the  $\phi$  radiative decay  $\phi \rightarrow f_0(980)\gamma \rightarrow \pi^+\pi^-\gamma$ . Also in this case we deduce the contribution from Monte-Carlo simulation. This  $\phi$  decay is very interesting in itself and we report in the following section on a recent KLOE fit<sup>8</sup> of the mass spectrum for  $f_0(980) \rightarrow \pi^+\pi^-$ , using different theoretical models for the decay amplitude as well as a measurement of the charge asymmetry.

The analysis using tagged photons is in an advanced state. As in the published small photon angle analysis, we are studying the selection efficiencies (trigger, tracking, vertex, photon detec-

tion) directly from data using independent control samples. We find an overall good agreement with the predictions from simulation. While the trigger inefficiency is below 0.1%, we find values for the vertex efficiency and tracking efficiency of 99.2% and  $\sim 98\%$ , respectively. The total selection efficiency (not taking into account the geometrical acceptance) is 80 – 90% and rather flat in  $M_{\pi\pi}$ .

The  $\pi^+\pi^-\gamma$  event yield after application of all selection cuts is shown in fig. 1(right). As can be seen, the threshold region is covered in the large angle analysis and the huge background from  $\phi \rightarrow \pi^+\pi^-\pi^0$  can be considerably reduced. No corrections for  $\phi \rightarrow f_0(980)\gamma \rightarrow \pi^+\pi^-\gamma$  are yet applied in this plot, while FSR corrections are taken into account and the background from  $\mu^+\mu^-\gamma$  and  $\pi^+\pi^-\pi^0$  is subtracted.

As stressed above, the main limitation of the large angle analysis is due to the background associated with the  $\phi$ -decays into  $\pi^+\pi^-\pi^0$  and to  $f_0(980)\gamma$ . In order to reduce the systematic errors associated to these channels to a very low level, the DAΦNE collider has recently taken data off-resonance at a center-of-mass energy of  $\sqrt{s} = 1.00\text{GeV}$  (December 2005 to March 2006,  $250\text{pb}^{-1}$  integrated luminosity). The analysis of these data will allow an improved determination of the threshold region. Moreover, together with the data taken on-peak it will be possible to study the interference of the  $f_0(980)$  amplitude with FSR.

### 3 Study of the reaction $f_0(980) \rightarrow \pi^+\pi^-$

The scalar mesons  $f_0(980)$  and  $a_0(980)$  are produced at DAΦNE in radiative decays of the  $\phi$  meson and the study of these decays has caused much attention due to the potential sensitivity to distinguish between different models for the nature of the scalars ( $q\bar{q}$ , KK molecule, 4-quark)<sup>9</sup>. In the charged final state  $\phi \rightarrow f_0(980)\gamma \rightarrow \pi^+\pi^-\gamma$  the main background is arising from ISR and FSR continuum events  $e^+e^- \rightarrow \pi^+\pi^-\gamma$ . In order to reduce as much as possible the ISR contribution and in order to enhance the relative amount of the  $f_0(980)$  signal, the photon is required to be detected at large polar angles. The selection is therefore identical to the large photon angle analysis discussed above.

The  $M_{\pi\pi}$  spectrum is fitted with a function assuming the following contributions:  $f_0(980)$ , ISR, FSR, FSR- $f_0(980)$ -interference and  $\rho\pi$ , where the latter two arise from the interference between the FSR- and the  $f_0(980)$ -amplitude and from the decay chain  $\phi \rightarrow \rho\pi \rightarrow \pi^+\pi^-\gamma$ , respectively. The fit clearly prefers a negative interference between FSR and the scalar amplitude, for which three theoretical models have been used: (i) the kaon-loop (KL) model described in ref.<sup>10</sup>, (ii) the no-structure (NS) model of ref.<sup>11</sup> and (iii) the scattering-amplitude model (SA) of ref.<sup>12</sup>. Further details concerning these models can be found in the appropriate references. Free parameters concerning the scalar amplitudes are the mass of the  $f_0(980)$ , the couplings  $f_0K^+K^-$ ,  $f_0\pi^+\pi^-$  (for KL and NS) and the direct coupling  $\phi f_0\gamma$  (for NS). In the case of the SA model, in which the scalar amplitude is the sum of the  $\pi\pi \rightarrow \pi\pi$  and  $\pi\pi \rightarrow KK$  scattering amplitudes, the fit parameters are an overall phase and the 6 coefficients of an expansion, which parametrize the mass dependence of the two scattering amplitudes.

We fit the data in the region  $420 < M_{\pi\pi} < 1010$  MeV using bins 1.2 MeV wide. The results of the fit are shown in fig. 2 for the KL and NS models. The  $f_0(980)$  signal appears as an excess of events in the region between 900 and 1000 MeV. An attempt to include a second scalar meson, namely the  $f_0(600)$ , does not improve the fit quality. After subtraction of the non-scalar part, an asymmetric peak around 980 MeV with a FWHM of 30 – 50 MeV is obtained, as shown in fig. 2 in the lower row. Such a peak does not directly represent the  $f_0(980)$  shape but it results from the sum of the broad signal amplitude and the negative interference term that cancels the low mass tail. The ratio of the  $f_0K^+K^-$  and  $f_0\pi^+\pi^-$  couplings  $R = g_{f_0K^+K^-}^2/g_{f_0\pi^+\pi^-}^2$  is well above 2 (KL: 2.2 – 2.8, NS: 2.6 – 4.4), indicating a strong coupling of the  $f_0(980)$  to strangeness. For the SA fit, which has a worse fit quality, we find only marginal agreement with

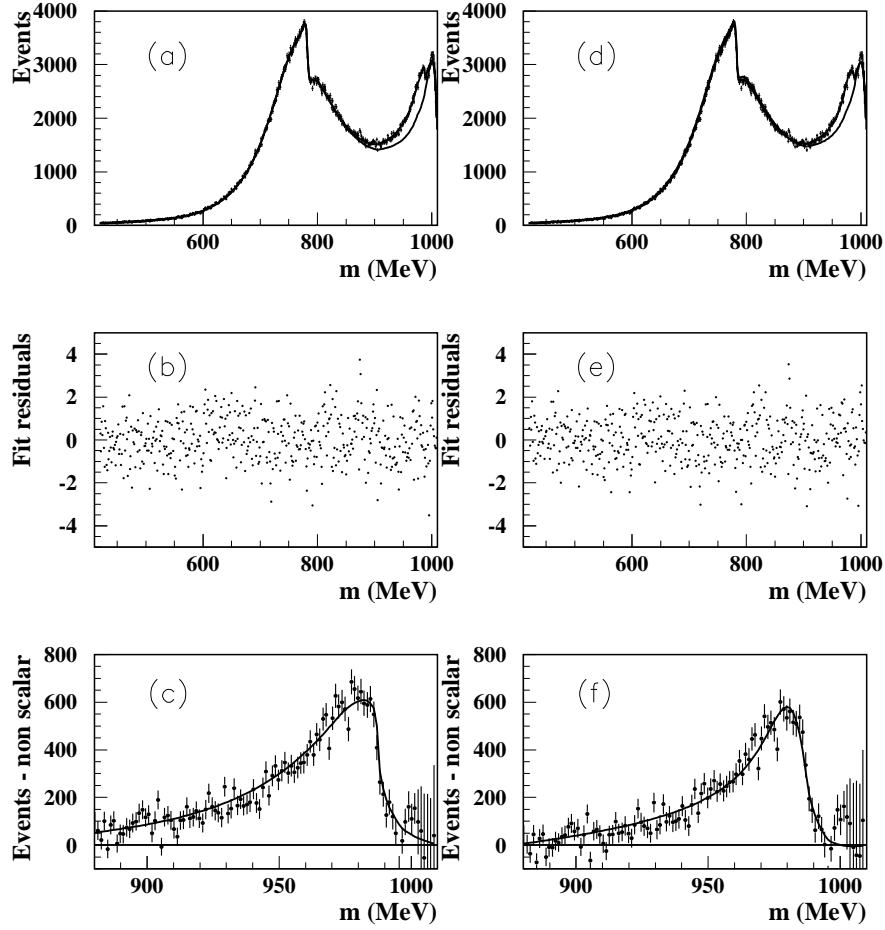


Figure 2: *Result of the KL fit (a)-(b)-(c) and of the NS fit (d)-(e)-(f). (a)-(d) Data spectrum compared with the fitting function (upper curve following the data points) and with the estimated non-scalar part of the function (lower curve); (b)-(e) fit residuals as a function of  $m$ ; (c)-(f) the fitting function is compared to the spectrum obtained subtracting to the measured data the non-scalar part of the function in the  $f_0$  region.*

the KL and NS results. Especially the branching ratio  $\text{BR}(\phi \rightarrow f_0 \gamma) \times \text{BR}(f_0 \rightarrow \pi^+ \pi^-)$  can be extracted and is found to be in the order  $10^{-5}$ , being about one order of magnitude lower than the values extracted from the KL and NS parameters. The complete list of fit results and further information concerning the procedure can be found in ref. <sup>8</sup>.

As proposed in ref. <sup>13</sup>, the behaviour of the forward-backward asymmetry as a function of  $M_{\pi\pi}$  has been studied. The forward-backward asymmetry is defined as

$$A_c = \frac{N(\theta_{\pi^+} > 90^\circ) - N(\theta_{\pi^+} < 90^\circ)}{N(\theta_{\pi^+} > 90^\circ) + N(\theta_{\pi^+} < 90^\circ)}, \quad (1)$$

and is plotted in fig. 3 for data and for two Monte-Carlo predictions, excluding and including the presence of the  $f_0(980)$  amplitude. As can be seen from the plot, the inclusion of the scalar amplitude is necessary for an acceptable agreement at high and low masses. While at low masses the  $f_0(980)$  amplitude is cancelled in the mass spectrum due to the destructive interference with FSR, on the contrary the scalar amplitude is very evident in the charge asymmetry due to the interference with ISR.

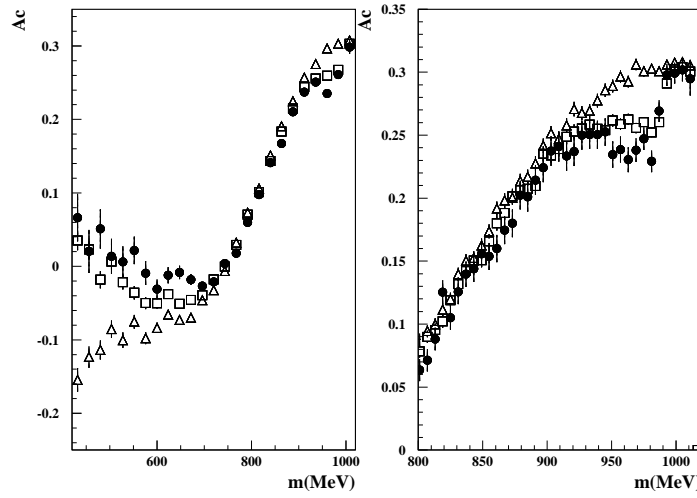


Figure 3: The forward-backward asymmetry for data (full circles) compared to the Monte-Carlo expectations based on the non-scalar part of the spectrum only (open triangles), and on the non-scalar plus  $f_0(980)$  part obtained from the KL amplitude (open squares). The right plot shows the detail of the comparison in the  $f_0$  mass region.

## References

1. G.W. Bennet *et al.* [E821 collaboration], Phys. Rev. **D73** (2006) 072003
2. S. Eidelman and F. Jegerlehner, Z.Phys. **C67** (1995) 585
3. M. Davier, S. Eidelman, A. Höcker and Z. Zhang, Eur. Phys. J. **C31**, (2003) 503; A. Höcker, hep-ph/0410081
4. A. Aloisio *et al.* [KLOE collaboration], Phys. Lett. **B606** (2005) 12
5. S. Binner, J.H. Kühn and K. Melnikov, Phys. Lett. B **459** (1999) 279; G. Rodrigo, A. Gehrmann-De Ridder, M. Guillaume and J.H. Kühn, Eur. Phys. J. **C22**, (2001) 81; G. Rodrigo, H. Czyż, J.H. Kühn and M. Szopa, Eur. Phys. J. **C24** (2002) 71; H. Czyż, A. Grzelińska, J. H. Kühn and G. Rodrigo, Eur. Phys. J. **C27**, (2003) 563; H. Czyż, A. Grzelińska, J. H. Kühn and G. Rodrigo, Eur. Phys. J. **C33**, (2004) 333; H. Czyż, A. Grzelińska, J. H. Kühn and G. Rodrigo, Eur. Phys. J. **C39**, (2005) 411; H. Czyż and E. Nowak-Kubat, Phys. Lett. **B634** (2006) 493
6. R.R. Akhmetshin *et al.* [CMD-2 collaboration], Phys. Lett. **B476** (2000) 33; R.R. Akhmetshin *et al.* [CMD-2 collaboration], Phys. Lett. **B527** (2002) 161
7. M.N.Achasov *et al.* [SND collaboration], Zh. Eksp. Teor. Fiz. **B128** (2005) 1201; M.N.Achasov *et al.* [SND collaboration], hep-ex/0605013
8. A. Aloisio *et al.* [KLOE collaboration], Phys. Lett. **B634** (2006) 148
9. N.N.Achasov and V.N.Ivanchenko, Nucl.Phys.**B315** (1989) 465; F.E.Close, N.Isgur and S.Kumano, Nucl.Phys. **B389** (1993) 513
10. N.N.Achasov and V.V.Gubin, Phys.Rev. **D57** (1998) 1987
11. G.Isidori, L.Maiani, M.Nicolaci and S.Pacetti, hep-ph/0603241
12. M.Boglione, M.R.Pennington, Eur. Phys. J. **C30** (2003) 503
13. H. Czyż, A. Grzelińska and J. H. Kühn, Phys. Lett. **B611** (2005) 116